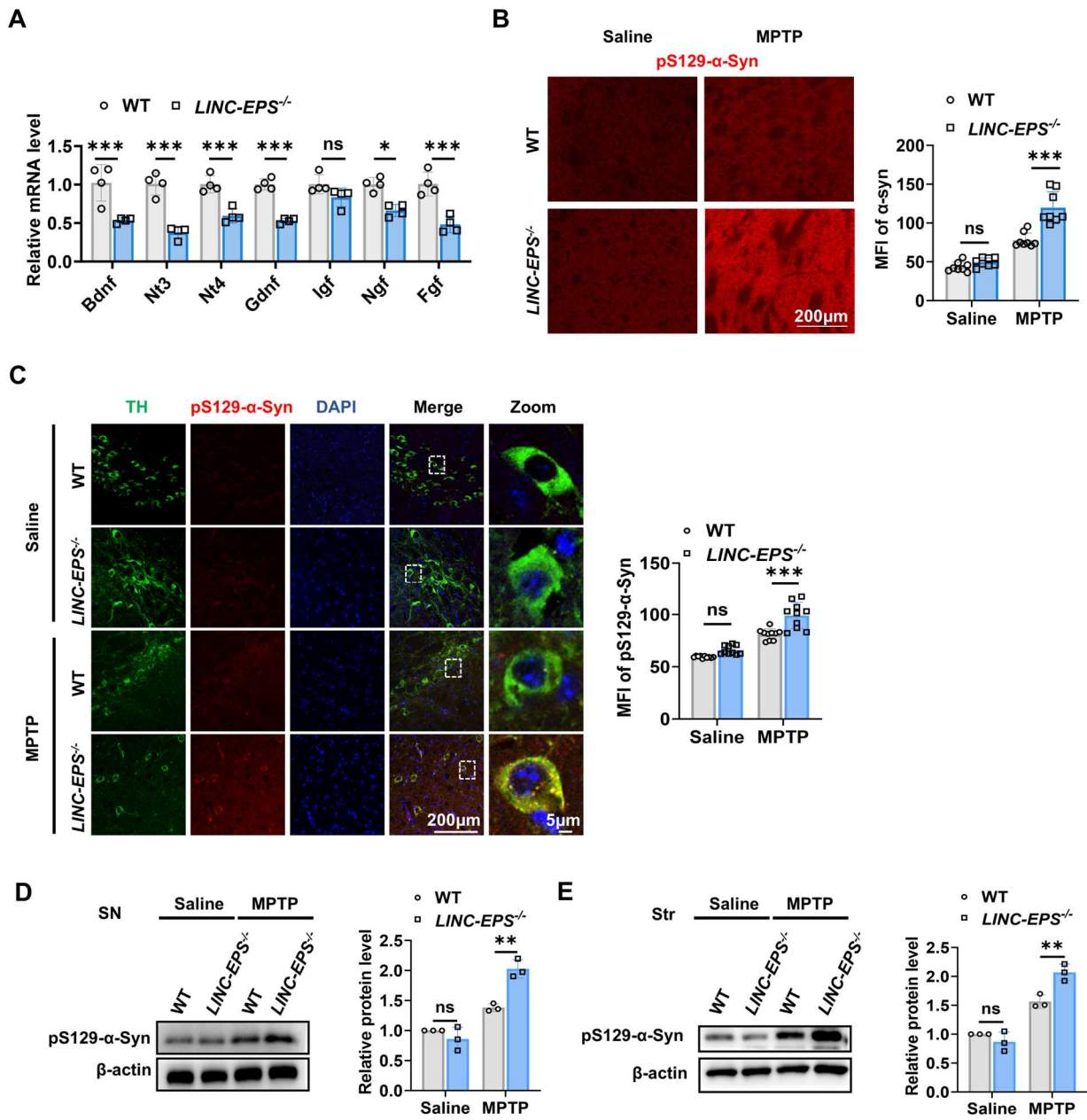


1 **Supplementary Figure Caption**

2 **Fig. S1**



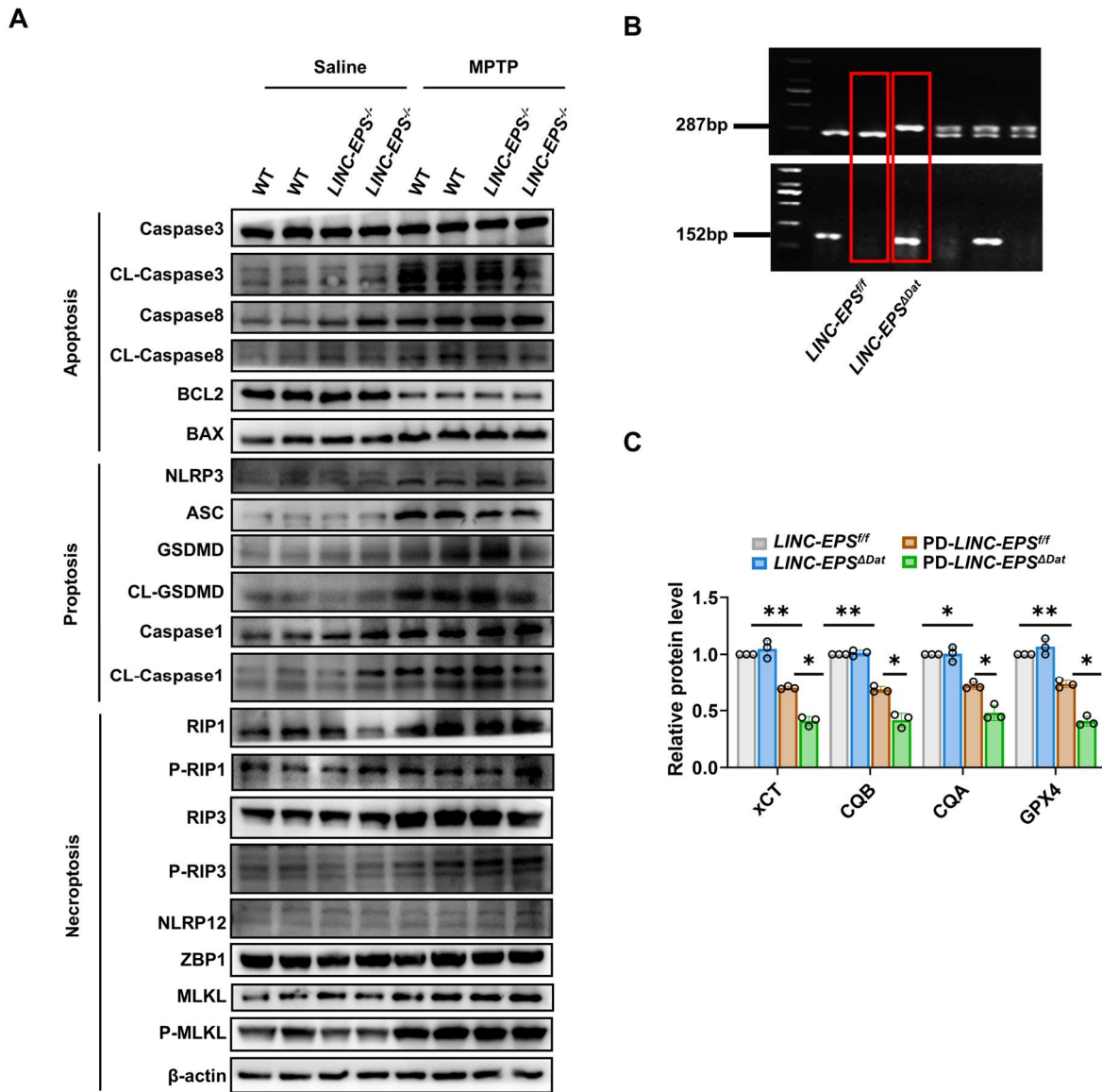
3

4 **Fig. S1 *LINC-EPS* Deficiency Exacerbates MPTP-Induced Neurochemical and Pathological**
 5 **Alterations**

6 **(A)** RT-qPCR analysis of neurotrophic factor mRNA levels (Bdnf, Nt3, Nt4, Gdnf, Igf, Ngf, Fgf) in
 7 midbrain tissue from the indicated groups (n = 4). **(B)** Representative immunofluorescence images of
 8 pS129- α -Syn (red) in the striatum and quantification of its mean fluorescence intensity (MFI) (n = 8).

9 Scale bar, 200 μm . **(C)** Representative co-immunofluorescence images for pS129- α -Syn (red), TH
10 (green), and DAPI (blue) in the SNpc. Right panels show magnified views of the boxed areas. Far
11 right: Quantification of pS129- α -Syn MFI within TH⁺ neurons (n = 10). Scale bar, 200 μm . **(D, E)**
12 Representative immunoblots and quantification of pS129- α -Syn protein levels in the SN **(D)** and
13 striatum **(E)**. β -actin served as a loading control (n = 3). Data are presented as mean \pm SEM. Statistical
14 significance was determined by two-way ANOVA with Tukey's post-hoc test. * $P < 0.05$, ** $P < 0.01$,
15 *** $P < 0.001$. ns, not significant.

16



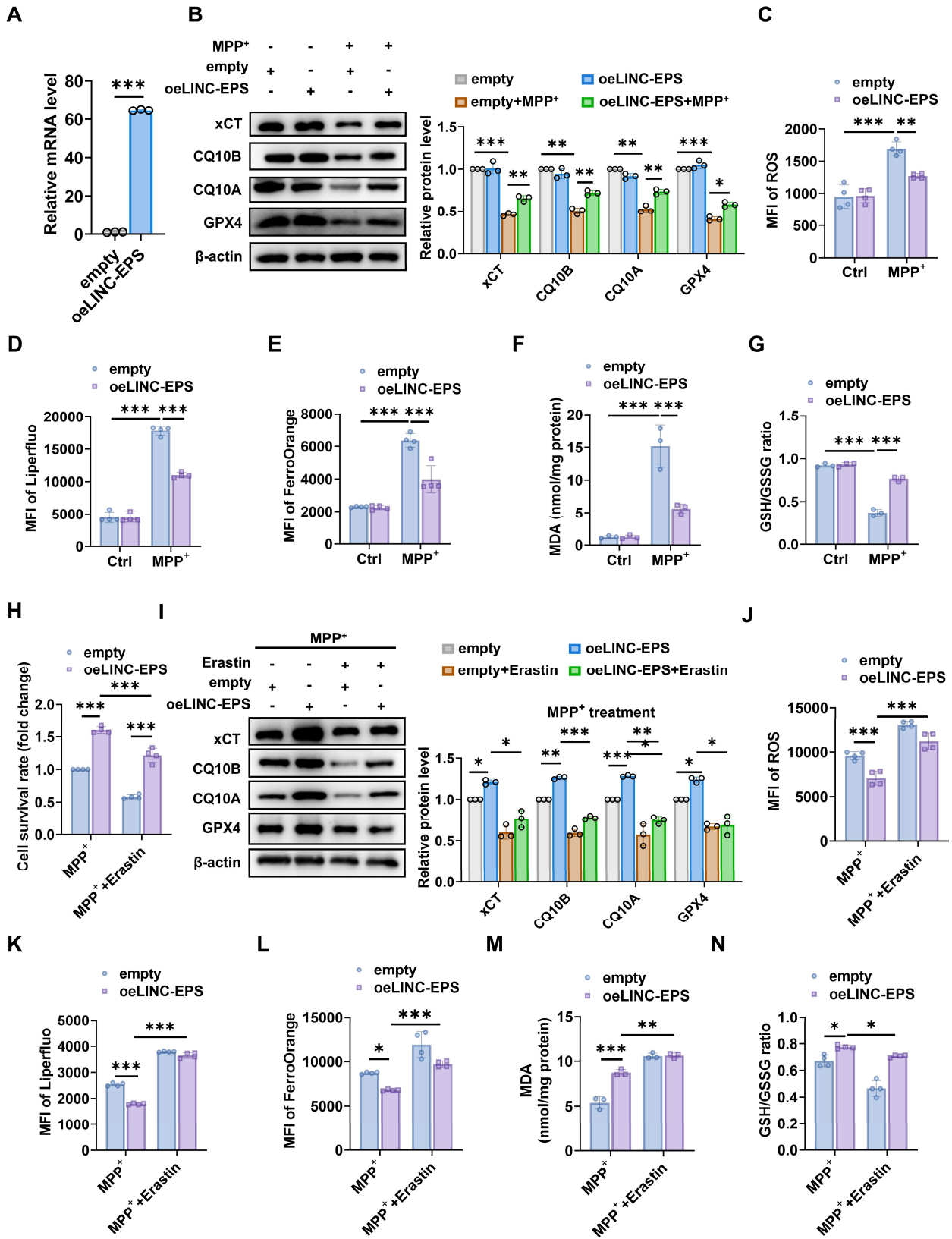
18

19 **Fig. S2 LINC-EPS Deficiency Does Not Activate Other Major Regulated Cell Death Pathways**

20 (A) Representative immunoblots of key protein markers for apoptosis (CL-Caspase-3), pyroptosis
 21 (CL- Caspase-1, GSDMD-N), and necroptosis (P-MLKL, P-RIP3) in primary neurons from WT and
 22 *LINC-EPS*^{-/-} mice treated with or without MPP⁺ (500 μM, 24 h). Due to limited primary neuron yield,
 23 two technical replicates from pooled neurons (six mice per pool). (B) Genotyping PCR validation of

24 dopamine neuron-specific LINC-EPS conditional knockout (*LINC-EPS^{ADat}*) mice. The 287 bp band
25 represents the floxed allele (loxP sites flanking the target region), and the 152 bp band indicates the
26 deleted allele after Cre-mediated excision of the intervening sequence. *LINC-EPS^{ff}* control mice
27 showed only the 287 bp floxed allele, whereas *LINC-EPS^{ADat}* mice displayed both the 287 bp band
28 (from non-recombined cells) and the 152 bp band (from dopaminergic neurons with successful Cre-
29 mediated deletion). (C) Quantification of relative protein levels for xCT, CQ10B, CQ10A and GPX4
30 from the immunoblots shown in Figure 3H (n = 3). Data are presented as mean ± SEM. Statistical
31 significance was determined using two-way ANOVA followed by Tukey's post hoc test. **P* < 0.05,
32 ***P* < 0.01, ****P* < 0.001; ns, not significant.

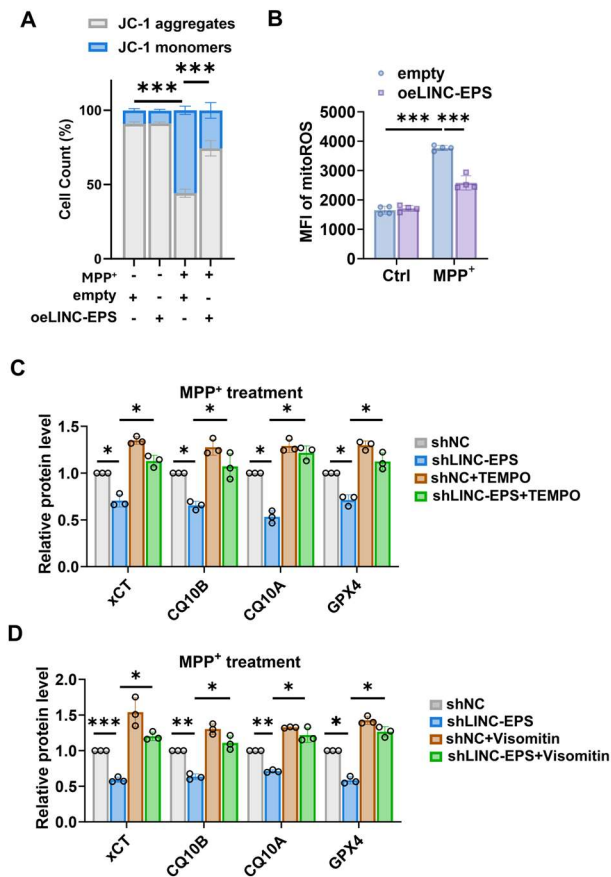
33



36 **Fig. S3 LINC-EPS overexpression protects SH-SY5Y cells from MPP⁺- and Erastin-induced**
37 **ferroptosis**

38 SH-SY5Y cells stably overexpressing LINC-EPS (oeLINC-EPS) or empty vector control were treated
39 with MPP⁺ (500 μ M, 24 h) with or without erastin (10 μ M, 24 h). **(A)** qRT-PCR validation of LINC-
40 EPS overexpression (n = 3). **(B–G)** Effects of LINC-EPS overexpression on MPP⁺-induced
41 ferroptosis: **(B)** protein levels of xCT, CQ10B, CQ10A, and GPX4 (n = 3); **(C)** total ROS (n = 4); **(D)**
42 lipid ROS (n = 4); **(E)** Fe²⁺ levels (n = 4); **(F)** MDA content (n = 3); **(G)** GSH/GSSG ratio (n = 3).
43 **(H–N)** Combined effects of LINC-EPS overexpression and erastin treatment: **(H)** cell viability (n =
44 4); **(I)** xCT, GPX4, CQ10A, and CQ10B protein levels (n = 3); **(J)** total ROS (n = 4); **(K)** lipid ROS
45 (n = 4); **(L)** Fe²⁺ levels (n = 4); **(M)** MDA content (n = 3); **(N)** GSH/GSSG ratio (n = 4). Data are
46 mean \pm SEM. Statistical analysis: two-tailed Student's t-test **(A)** or two-way ANOVA with Tukey's
47 post-hoc test **(B–N)**. **P* < 0.05, ***P* < 0.01, ****P* < 0.001. Detailed experimental procedures are
48 described in Materials and Methods.

49

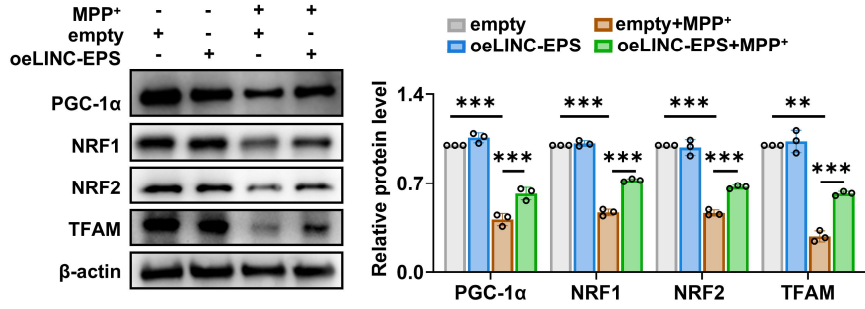


51

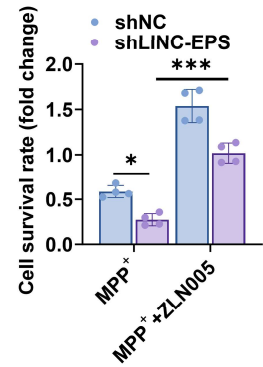
52 **Fig. S4 LINC-EPS Deficiency-Induced Ferroptotic Phenotypes are Rescued by mitoROS**53 **Scavengers**54 **(A, B)** oeLINC-EPS or empty cells were treated with or without MPP⁺ (500 μ M, 24 h). **(A)** Flow55 cytometry analysis of MMP (n = 4). **(B)** Quantification of mitoROS levels (n = 4). **(C)** Quantification56 of relative protein levels from immunoblots shown in Figure 6G (n = 3). **(D)** Quantification of relative57 protein levels from immunoblots shown in Figure 6H (n = 3). Data are presented as mean \pm SEM.58 Statistical significance was determined by two-way ANOVA with Tukey's post-hoc test. **P* < 0.05,59 ***P* < 0.01, ****P* < 0.001.

60

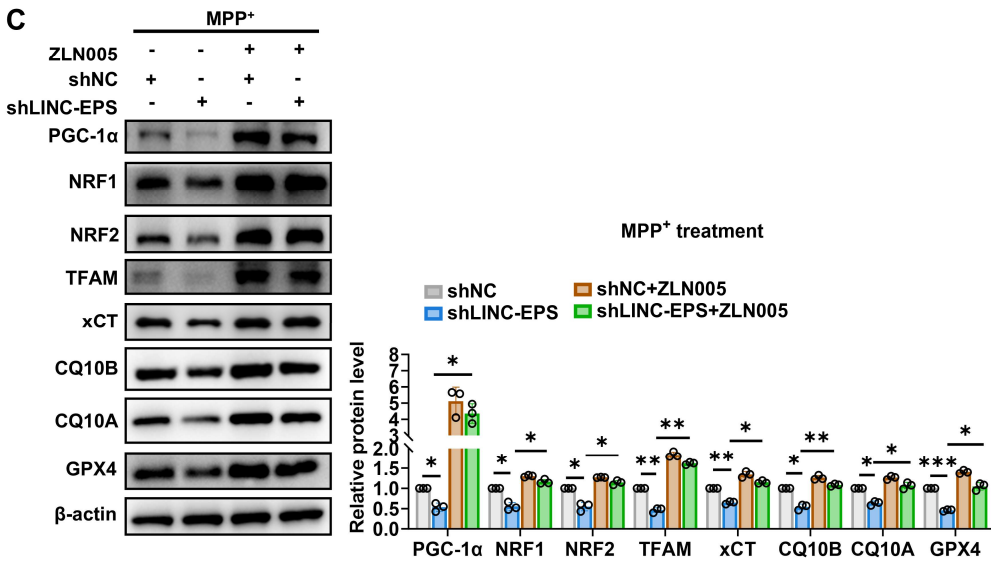
A



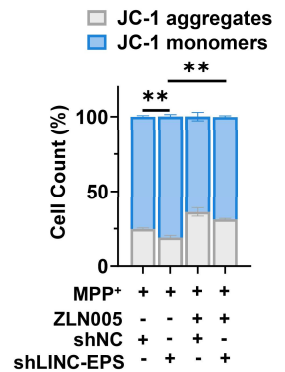
B



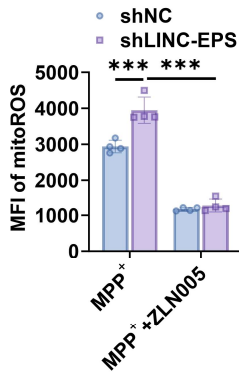
C



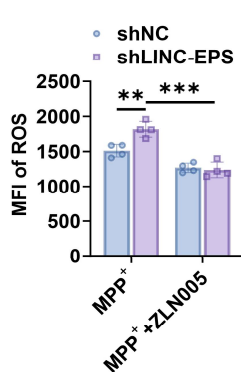
D



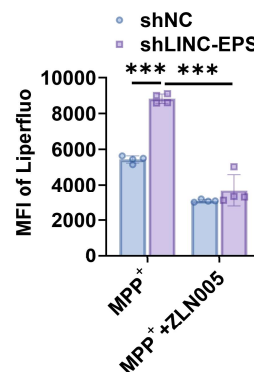
E



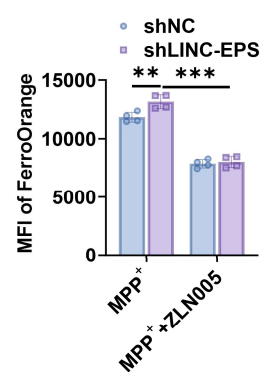
F



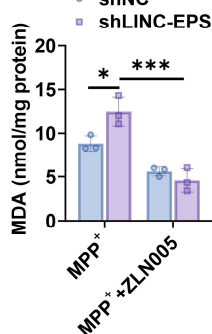
G



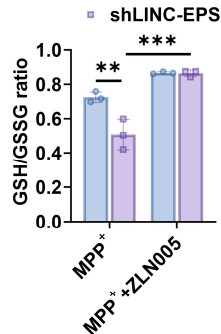
H



I



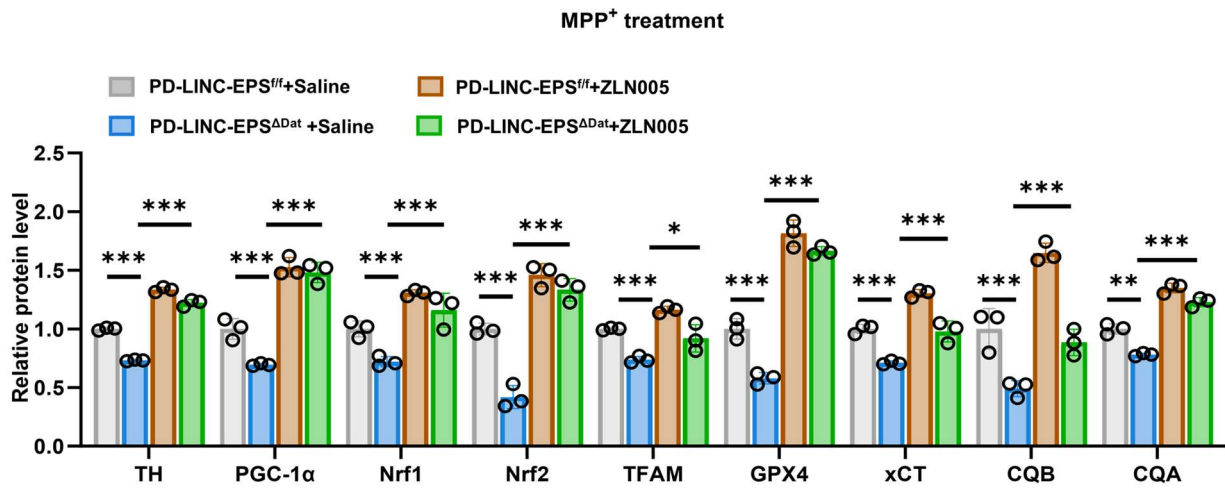
J



63 **Fig. S5 Pharmacological and Genetic Modulation of the LINC-EPS/PGC-1 α Axis**

64 **(A)** PGC-1 α axis protein expression in oeLINC-EPS or empty vector cells treated with or without
65 MPP⁺ (500 μ M, 24 h) (n = 3). **(B–J)** shLINC-EPS cells were treated with MPP⁺ (500 μ M, 24 h) with
66 or without the PGC-1 α agonist ZLN005 (10 μ M). **(B)** Cell viability (n = 4); **(C)** PGC-1 α axis and
67 ferroptosis defense protein levels (n = 3); **(D)** mitochondrial membrane potential (n = 4); **(E)** mitoROS
68 levels (n = 4); **(F)** total ROS (n = 4); **(G)** lipid ROS (n = 4); **(H)** Fe²⁺ levels (n = 4); **(I)** MDA content
69 (n = 3); **(J)** GSH/GSSG ratio (n = 3). Data are mean \pm SEM. Statistical analysis: two-way ANOVA
70 with Tukey's post-hoc test. **P* < 0.05, ***P* < 0.01, ****P* < 0.001. Detailed experimental procedures
71 are described in Materials and Methods.

72



74

75 **Fig. S6 Quantification of Protein Expression Levels in the Midbrain**

76 Quantification of the immunoblot analysis shown in Figure 9I for TH, PGC-1α, NRF1, NRF2, TFAM,
 77 GPX4, xCT, CQ10B, and CQ10A. Protein levels were normalized to β-actin (n = 3). Data are
 78 presented as mean ± SEM. Statistical significance was determined by two-way ANOVA with Tukey's
 79 post-hoc test. **P* < 0.05, ***P* < 0.01, ****P* < 0.001.

80

81 **Supplementary Materials and Methods**

82 **Immunohistochemistry and Imaging**

83 Following terminal anesthesia with Avertin (30 μ L/g, i.p.), animals were perfused transcardially
84 with ice-cold saline and subsequently with 4% paraformaldehyde (PFA). Excised brains were post-
85 fixed overnight in 4% PFA at 4°C, followed by cryoprotection in a 30% sucrose solution. Coronal
86 sections (15–30 μ m thickness) were then prepared using a Leica cryostat. For immunofluorescence
87 staining, free-floating sections were first permeabilized with 0.3% Triton X-100 and then blocked in
88 5% BSA. Subsequently, sections were incubated with primary antibodies in the Supplementary
89 Materials (Table S2) overnight at 4°C. After washing, sections were incubated with the appropriate
90 Alexa Fluor-conjugated secondary antibodies and nuclei were counterstained with DAPI.
91 Fluorescence signals were captured on a Zeiss LSM 880 confocal microscope, and subsequent image
92 analysis was performed using Fiji software (ImageJ).

93 **Western Blot Analysis**

94 For protein analysis, total lysates were extracted from cells or tissues using RIPA buffer
95 supplemented with protease and phosphatase inhibitors. Protein concentration was quantified via a
96 BCA assay. Equal protein quantities were resolved by SDS-PAGE and transferred to PVDF
97 membranes (Millipore). The membranes were subsequently blocked with 5% non-fat milk in TBST
98 and incubated overnight at 4°C with the indicated primary antibodies. Following incubation with
99 HRP-conjugated secondary antibodies (see Supplementary Table 2 for details), immunoreactive
100 bands were visualized using an ECL detection reagent and quantified by densitometry with ImageJ
101 software.

102 **Flow Cytometry and Fluorescence Probes**

103 Mitochondrial superoxide was detected using MitoSOX Red (MCE). General cellular ROS was
104 measured with a Dihydroethidium (DHE) probe (KeyGEN BioTECH). Mitochondrial membrane
105 potential was assessed using a JC-1 kit (Beyotime). Labile iron (Fe^{2+}) was detected with FerroOrange
106 (Dojindo), and lipid peroxidation was visualized with Liperfluo (Dojindo). Cells were stained
107 according to the manufacturers' protocols and analyzed on a CytoFLEX flow cytometer (Beckman
108 Coulter). MDA levels and the ratio of GSH/GSSG were measured using commercial kits from
109 Beyotime, following the manufacturer's instructions.

110 **RNA Isolation and Quantitative RT-PCR**

111 Total RNA was isolated from cultured cells or tissue samples using TRIzol reagent (Invitrogen).
112 Following the elimination of residual genomic DNA, complementary DNA (cDNA) was synthesized
113 from 1 μg of total RNA utilizing the HiScript III RT SuperMix (Vazyme). The quantification of
114 specific transcripts was subsequently performed by qPCR on a QuantStudio 5 system (Applied
115 Biosystems) with SYBR Green Master Mix (Vazyme). Relative gene expression levels were
116 determined using the $2^{-\Delta\Delta\text{Ct}}$ comparative threshold method, normalized to Actb (β -actin) as an
117 endogenous reference gene. The specific primer sequences employed for amplification are provided
118 in the Supplementary Materials (Table S5).

119 **RNA Immunoprecipitation (RIP)**

120 RNA immunoprecipitation (RIP) was conducted using the Magna RIP Kit (Millipore) in
121 accordance with the manufacturer's guidelines. Cell lysates were subjected to immunoprecipitation
122 with magnetic beads conjugated to either an anti-PGC-1 α antibody (Proteintech, Cat# 66369-1-Ig) or
123 a control IgG. Following stringent washing steps to remove non-specific binding, the co-precipitated
124 RNA was isolated and subsequently quantified by RT-qPCR.

125 Chromatin Isolation by RNA Purification (ChIRP)

126 ChIRP was performed using the Magna ChIRP RNA Interactome Kit (Millipore). SH-SY5Y
127 cells were cross-linked with 1% formaldehyde. Chromatin was sonicated to an average size of 200-
128 500 bp. Biotinylated probes targeting LINC-EPS or LacZ (negative control) were hybridized with the
129 chromatin lysate. The probe-chromatin complexes were captured with streptavidin magnetic beads.
130 After washing and elution, the associated DNA was purified and analyzed by qPCR.

131 RNA Pull-down Assay

132 Biotinylated LINC-EPS and antisense control probes were transcribed *in vitro* (T7 RiboMAX,
133 Promega). Probes were bound to streptavidin magnetic beads (Invitrogen) and incubated with SH-
134 SY5Y cell lysates. After washing, bound proteins were eluted and analyzed by Western blotting.

135 Lentivirus Production and Infection

136 Lentiviral vectors for LINC-EPS overexpression (pLV-LINC-EPS) and knockdown (sh-LINC-
137 EPS; target sequence: GCCCCCTGCCCTGCCCACTG) were constructed by Tsingke Biotechnology
138 (Beijing, China). Empty vector (empty) and non-targeting shRNA (shNC) served as controls.
139 Lentivirus was produced by co-transfecting 293T cells with the transfer plasmid and packaging
140 plasmids (psPAX2, pMD2.G) using Lipofectamine 8000 (Thermo Fisher). Viral supernatants were
141 collected, filtered (0.45 μm), and used to infect SH-SY5Y cells in the presence of polybrene (8
142 $\mu\text{g/mL}$). Stable cell lines were selected using puromycin (2 $\mu\text{g/mL}$; Sigma-Aldrich).

143 Dual-Luciferase Reporter Assay

144 The putative TBE was amplified from genomic DNA and inserted in either forward (TBE-F) or
145 reverse (TBE-R) orientation downstream of a Ppargc1a promoter-luciferase cassette (2 kb upstream
146 of the transcription start site, cloned into pGL3-basic; Promega). Control constructs included pGL3-

147 basic alone and pGL3 constructs containing TBE sequences without the Ppargc1a promoter. All
148 plasmids were verified by Sanger sequencing.

149 SH-SY5Y cells were transiently co-transfected with a firefly luciferase reporter construct (500
150 ng) and a pRL-TK Renilla luciferase normalization control vector (50 ng; Promega), utilizing
151 Lipofectamine 3000 (Invitrogen). Twenty-four hours post-transfection, cells were subjected to the
152 indicated treatments prior to lysis. The luminescence from both luciferases was quantified using the
153 Dual-Luciferase Reporter Assay System (Promega) with a GloMax 96 microplate luminometer. To
154 control for transfection efficiency, firefly luciferase activity was normalized to the corresponding
155 Renilla luciferase activity.

156

157

158 **Supplementary Table**159 **Table S1. The main reagents and kits**

Product Name	Supplier	Catalog Number (if available)
Chemicals and Inhibitors		
MPTP	Sigma-Aldrich (St. Louis, MO, USA)	M0896
MPP ⁺ iodide	Sigma-Aldrich (St. Louis, MO, USA)	D048
Ferrostatin-1	MCE (Monmouth Junction, NJ, USA)	HY-100579
Necrostatin-1	MCE (Monmouth Junction, NJ, USA)	HY-15760
Z-VAD-FMK	MCE (Monmouth Junction, NJ, USA)	HY-16658B
Mito-TEMPO	MCE (Monmouth Junction, NJ, USA)	HY-112879
Visomitin (SkQ1)	MCE (Monmouth Junction, NJ, USA)	HY-112130
Cell Culture and Transfection		
DMEM, high glucose	Servicebio (Wuhan, China)	G4510
Fetal Bovine Serum (FBS)	Gibco (Grand Island, NY, USA)	10099141
Penicillin-Streptomycin Solution	Beyotime (Shanghai, China)	C0222

Opti-MEM I Reduced Serum Medium	Gibco (Grand Island, NY, USA)	31985070
Molecular Biology Kits		
AccuRT-SuperMix	Accurate Biology (Hunan, China)	AG11728
RIPA Lysis Buffer	KeyGEN BioTECH (Jiangsu, China)	KGP702
BCA Protein Assay Kit	Solarbio (Beijing, China)	PC0020
SDS-PAGE Gel Preparation Kit	U-landy (Suzhou, China)	
Protein A/G Magnetic Beads	MCE (Monmouth Junction, NJ, USA)	HY-K0202
Western Blotting Reagents		
PVDF Membrane, 0.45 μm	Millipore (Billerica, MA, USA)	IPVH00010
NcmColor Prestained Protein Ladder	NCM Biotech (Suzhou, China)	
Non-fat Dry Milk	Lanjieke Tech (China)	
Tris, Glycine, SDS, Tween-20	Solarbio (Beijing, China)	
Fluorescent Probes and Assay Kits		
		HY-D0942
MitoSOX™ Red Indicator	MCE (Monmouth Junction, NJ, USA)	(from Invitrogen)

DHE (ROS) Detection Kit	KeyGEN BioTECH (Jiangsu, China)	KGAF019
FerroOrange	Dojindo (Kumamoto, Japan)	F374
Liperfluo	Dojindo (Kumamoto, Japan)	L248
Mitochondrial Membrane Potential Kit (JC-1)	Beyotime (Shanghai, China)	C2006
MDA Assay Kit	Beyotime (Shanghai, China)	S0131S
GSH and GSSG Assay Kit	Beyotime (Shanghai, China)	S0053

160

161 **Table S2 The main antibodies**

Antibody name	Manufacturer	Product Number	Dilution ratio (WB)	Dilution ratio (IF/IP)	Dilution ratio (IP/RIP/MER IP)
TH	Servicebio	GB11181-100	1:500	1:200	
TH	Servicebio	GB12181-100	1:500	1:200	
xCT	Servicebio	GB115276-100	1: 500		
α -Syn	CST	45083SF	1:1000	1:200	
p53	CST	9238	1:1000		
Bcl-2	CST	3948	1:1000		
β -Actin	CST	3700S	1:1000		

GPX4	HUABIO	AB_3070665	1:10000	1:100
GPX4	ABclonal	A13309	1:1000	1:100
CQ10B	UpingBio	YP-mAb-18654	1:1000	
CQ10A	UpingBio	YP-mAb-09554	1:1000	
FTL	Proteintech	10727-1-AP	1:1000	
FSP1	Proteintech	20886-1-AP	1:1000	
Bax	CST	2772	1:1000	
Gasdermin D	CST	39754	1:1000	
GFAP	Abcam	ab7260	1:1000	
Iba1	WAKO	019-19741	1:1000	
ASC	CST	67824	1:1000	
Phospho-RIP1 (Ser166)	CST	31122	1:1000	
Phospho-RIP3 (Ser227)	CST	91702	1:1000	
PGC-1 α	Proteintech	66369-1-Ig	1:1000	1:25
ZBP1	Proteintech	13285-1-AP	1:1000	
RIPK1	CST	3493	1:1000	
RIPK3	CST	15828	1:1000	

NLRP12	Cusabio	CSB- PA015867GA01 HU	1:1000
CL-Casp1	CST	89332	1:1000
Casp1	CST	83383	1:1000
CL-GSDMD	CST	10137	1:1000
CL-Casp3	CST	9664	1:1000
Casp3	CST	14220	1:1000
p-MLKL	CST	37333	1:1000
MLKL	CST	26539	1:1000
CL-Casp8	CST	8592	1:1000
Casp8	CST	4790	1:1000
NLRP3	CST	15101	1:1000
HRP-conjugated Goat Anti-Rabbit IgG(H+L)	Proteintech	SA00001-2	1:10000
HRP-conjugated Goat Anti-Mouse IgG(H+L)	Proteintech	SA00001-1	1:10000
Multi-rAb™	Proteintech	RGAR011	1:10000

Polymer HRP-

Goat Anti-Rabbit

Multi-rAb™ Proteintech RGAR002 1:200

CoraLite® Plus

488-Goat Anti-

Rabbit

Multi-rAb™ Proteintech RGAM002 1:200

CoraLite® Plus

488-Goat Anti-

Mouse

Multi-rAb™ Proteintech RGAR004 1:200

CoraLite® Plus

594-Goat Anti-

Rabbit

Multi-rAb™ Proteintech RGAM004 1:200

CoraLite® Plus

594-Goat Anti-

Mouse

Multi-rAb™ Proteintech RGAR005 1:200

CoraLite® Plus

647-Goat Anti-

Rabbit

Multi-rAb™ Proteintech RGAM005 1:200
CoraLite® Plus
647-Goat Anti-
Mouse

162

163 **Table S3: Human blood sample information**

164

HD		
Sample	Gender: 1 male and 2 females	Age
1	2	39
2	2	87
3	2	53
4	1	38
5	1	38
6	1	72
7	1	59
8	2	50
9	2	75
10	2	70

11	2	56
12	1	64
13	2	62
14	1	48
15	1	76
16	2	71
17	1	42
18	2	87
19	1	66
20	2	63
21	2	56
22	2	57
23	1	57
24	2	42
25	1	57
26	2	56
27	1	56
28	1	25

29 1 56

30 1 78

PD

Sample	Course of the disease (years)	Gender: 1 male and 2 females	Age	UPDRS-III
1	5	1	63	33
2	11	1	77	18
3	4.5	2	68	19
4	0.5	2	76	13
5	2	1	66	19
6	7	2	65	12
7	1	2	76	21
8	11	1	72	20
9	4	1	62	20
10	1.5	1	70	32
11	2	2	71	16
12	5	2	63	28
13	9	1	70	23
14	1	1	60	2
15	6	1	60	6
16	3	1	65	6
17	4	2	67	29
18	1	1	67	16
19	2	2	63	15
20	1.5	2	52	26

21	1	1	78	8
22	10	2	77	28
23	3	1	60	12
24	1	1	61	8
25	2	1	53	13
26	2	2	62	13
27	1	1	75	10
28	6	2	74	12
29	10	1	80	26
30	11	1	82	29

166

167 **Table S4-1 Primer sequences for mouse tail identification**

Primer name	Upstream sequence	Downstream sequence
LINC-EPS-1	GCAGACAGGCGTGGACATTC	GCTTGTACTCGCCTCTTCTCTGCA
	ATTCT	A
LINC-EPS-2	TCACTGAATACACAGGCTGCT	GCTTGTACTCGCCTCTTCTCTGCA
	GCAA	A
Primer name	Upstream sequence	Downstream sequence
<i>LINC-EPS^{ff}</i>	CCTTAACAAATGTGGTCGCAT	CAACCCCAACCAGCAGATAAAG
	ACC	
<i>DAT^{Cre}</i>	TGGCTGTTGGTGTAAGTGG	GGACAGGGACATGGTTGACT

168

169 **Table S4-2 PCR Sample Loading System**

Component	Volume
Forward Primer (10 μ M)	1 μ L
Reverse Primer (10 μ M)	1 μ L
DNA	1.5 μ L
2 \times Taq PCR Master Mix	12.5 μ L
ddH ₂ O	9 μ L

170

171 **Table S4-3 PCR Program**

Stage	temperature	time	cycle number
Stage 1	95°C	5 min	1
	95°C	30 s	
Stage 2	60°C	30 s	35
	72°C	45 s	
Stage 3	Default instrument	Settings of the	1

172

173

174

175 **Table S5 The primer sequences**

Primer name	Upstream sequence	Downstream sequence
GAPDH	AAATCCCATCACCATCTTCCAG	AGGGGCCATCCACAGTCTTCT
m-LINC- EPS	GCGCACTTCTCTCATCTGTG	TCAGCTGTAGGATGGGAGGT
h-LINC- EPS	CGCATTAATGGGGGCATTCG	CTAAACCGTTTTCCCCGC
Bdnf	ATGGCGTTTCTCCGAAGCAT	TCCGCCCTATAAGCATCTTGA
Nt3	CCGTGGCATCCAAGGTAACAA	GCAGTTCGGTGTCCATTGC
Nt4	CTGTGTGCGATGCAGTCAGT	TGCAGCGGGTTTCAAAGAAGT
Gdnf	GGCAGTGCTTCCTAGAAGAGA	AAGACACAACCCCGGTTTTTG
Igf	GCTCTTCAGTTCGTGTGTGGA	GCCTCCTTAGATCACAGCTCC
Ngf	GGCAGACCCGCAACATTACT	CACCACCGACCTCGAAGTC
Fgf	CAGGCGGAGGCAGCTATAC	CCTGGTTCCTGGATAGTACC
PGC-1 α	GCTTTCTGGGTGGACTCAAGT	GAGGGCAATCCGTCTTCATCC
NRF1	AGGAACACGGAGTGACCCAA	TATGCTCGGTGTAAGTAGCCA
NRF2	TCAGCGACGGAAAGAGTATGA	CCACTGGTTTCTGACTGGATGT
TFAM	ATGGCGTTTCTCCGAAGCAT	TCCGCCCTATAAGCATCTTGA
MFN1	TGGCTAAGAAGGCGATTACTGC	TCTCCGAGATAGCACCTCACC
MFN2	CTCTCGATGCAACTCTATCGTC	TCCTGTACGTGTCTTCAAGGAA

OPA1	TGTGAGGTCTGCCAGTCTTTA	TGTCCTTAATTGGGGTCGTTG
DNM1L	CTGCCTCAAATCGTCGTAGTG	GAGGTCTCCGGGTGACAATTC
FIS1	AGCGGGATTACGTCTTCTACC	CATGCCACGAGTCCATCTTT
MFF	ACTGAAGGCATTAGTCAGCGA	TCCTGCTACAACAATCCTCTCC
PINK1	CCCAAGCAACTAGCCCCTC	GGCAGCACATCAGGGTAGTC
Parkin	GTGTTTGTTCAGGTTCAACTCCA	GAAAATCACACGCAACTGGTC
MT-ND1	GGCTATATACTACTACGCAAAGGC	GGTAGATGTGGCGGGTTTTAGG
MT-ND3	CCACAACCTAACGGCTACATAGAA	GGGTAAAAGGAGGGCAATTTCT
	A	AGA
MT-ND6	CAAACAATGTTCAACCAGTAACCA	ATATACTACAGCGATGGCTATTG
	CTAC	AGGA
NDUFA3	GGGGCCTCGCTGTAATTCTG	GACGGGCACTGGGTAGTTG
MT-CYB	ATCACTCGAGACGTAAATTATGGCT	TGAACTAGGTCTGTCCCAATGT
		ATG
ATP5F1A	GTATTGCCCGCGTACATGG	AGGACATACCCTTTAAGCCTGA
MT-ATP6	TAGCCATACACAACACTAAAGGAC	GGGCATTTTAAATCTTAGAGCG
	GA	AAA

176

177 **Table S6 The English abbreviations and full names that appear in the article**

Abbreviation	Full name
CHIRP	Chromatin Isolation by RNA Purification

Act-D	Actinomycin D
ChIP	Chromatin Immunoprecipitation
CHX	Cycloheximide
CCK-8	Cell Counting Kit-8
DAT	Dopamine Transporter
DAPI	4',6-diamidino-2-phenylindole
DA neurons	Dopaminergic neurons
DFO	Deferoxamine
Fe ²⁺	Ferrous iron
FISH	Fluorescence <i>in situ</i> hybridization
GSEA	Gene Set Enrichment Analysis
GPX4	Glutathione peroxidase 4
GSH	Glutathione (reduced form)

GSSG	Glutathione disulfide (oxidized form)
IF	Immunofluorescence
IP	Immunoprecipitation
JC-1	5,5',6,6'-tetrachloro-1,1',3,3'- tetraethylbenzimidazolylcarbocyanine iodide
KEGG	Kyoto Encyclopedia of Genes and Genomes
KO	Knockout
LINC-EPS	Long intergenic non-coding RNA-Enhancer of Polycomb-like protein
MDA	Malondialdehyde
MMP	Mitochondrial membrane potential
MPP ⁺	1-methyl-4-phenylpyridinium
MPTP	1-methyl-4-phenyl-1,2,3,6-tetrahydropyridine
mitoROS	Mitochondrial reactive oxygen species
NRF1	Nuclear respiratory factor 1
NRF2	Nuclear factor erythroid 2-related factor 2

oeLINC-EPS	Overexpression of lncRNA-EPS
oeNC	Overexpression negative control
PD	Parkinson's disease
PGC-1 α	Peroxisome proliferator-activated receptor- gamma coactivator 1-alpha
qRT-PCR	Quantitative real-time polymerase chain reaction
RIP	RNA Immunoprecipitation
ROS	Reactive oxygen species
SEM	Standard error of the mean
shLINC-EPS	Short hairpin RNA targeting lncRNA-EPS
shNC	Non-targeting control short hairpin RNA
SNpc	Substantia nigra pars compacta
TBE	T-box element
TEAD	TEA domain family member
TEM	Transmission electron microscopy

TH	Tyrosine hydroxylase
TFAM	Mitochondrial transcription factor A
WT	Wild-type
xCT	Solute Carrier Family 7 Member 11 (SLC7A11)
FSP1	Ferroptosis suppressor protein 1 (AIFM2)
FTL	Ferritin Light Polypeptide
ZLN005	A specific agonist of PGC-1 α

178

179